A NOVEL MULTI-DIMENSIONAL IIR NOTCH FILTER FOR ATTENUATING MULTIPLE NARROWBAND INTERFERENCES

Pattiya Kumburage Tharindu Chandima

(168453J)

Degree of Master of Science in Electronics and Automation

Department of Electronic and Telecommunication Engineering

University of Moratuwa

Sri Lanka

March 2021

A NOVEL MULTI-DIMENSIONAL IIR NOTCH FILTER FOR ATTENUATING MULTIPLE NARROWBAND INTERFERENCES

Pattiya Kumburage Tharindu Chandima

(168453J)

Dissertation submitted in partial fulfilment of the requirements for the

Master of Science in Electronics and Automation

Department of Electronic and Telecommunication Engineering

University of Moratuwa

Sri Lanka

March 2021

DECLARATION

"I declare that, this is my own work and this dissertation does not incorporate without acknowledgement any material previously submitted for a Degree or Diploma in any other University or institute of higher learning and to the best of my knowledge and belief it does not contain any material previously published or written by another person except where the acknowledgement is made in the text.

Also, I hereby grant to University of Moratuwa the non-exclusive right to reproduce and distribute my dissertation, in whole or in part in print, electronic or other medium. I retain the right to use this content in whole or part in future works (such as articles or books).

Signature: Date:

The above candidate has carried out research for the Masters dissertation under my supervision.

Name of the supervisor: Dr. Chamira U. S. Edussooriya

Signature of the supervisor: Date:

ABSTRACT

Notch filters are a class of filters that are used to attenuate narrowband interferences. Previously reported finite impulse response (FIR) or infinite impulse response (IIR) notch filters are predominantly limited to one-dimensional (1-D) or two-dimensional (2-D) signals. With emerging multi-dimensional (M-D) signals, such as four-dimensional (4-D) light fields and five-dimensional (5-D) light field videos, design techniques for M-D notch filters, beyond 2-D notch filters, are required to be investigated.

In this dissertation, a novel M-D multi notch IIR filter is proposed to attenuate multiple narrowband interferences. The structure of the notch filter is derived by cascading notch filter pairs. Initially, 1-D filter structure is presented and afterwards it is expanded as an M-D filter. The key factor of the proposed notch filter is the flexibility of placing the notches, adding any number of notches in to M-D and bandwidth can be controlled independently.

Narrowband interference attenuation has been verified using monochromatic image and a video. Capabilities of the proposed filter are compared against the existing filtering method using unity three-dimensional (3-D) signal. It is clearly noticeable that, the proposed M-D multi notch IIR filter has better performance as well as greater flexibility.

DEDICATION

To my parents

Rohana Pattiya Kumburage and Ramya Thejani Pattiya Kumburage

ACKNOWLEDGMENTS

I would like to express my sincere gratitude to my supervisor Dr. Chamira U. S. Edussooriya, Senior Lecturer, Department of Electronic and Telecommunication Engineering, University of Moratuwa for his immense guidance and invaluable advices given throughout the research. This research cannot be achieved without his enormous support by providing the precious knowledge and other valuable resources.

Next, I am grateful to express special thanks to parents, wife and parents-in-law for their admirable support and for encouraging me towards the completion of the work.

Also, I take this opportunity to thank the teachers for inspiring me throughout my entire journey.

If I had not had companionship with a nice group of humans: my office colleagues and friends, life would have been dull and boring.

Finally, I greatly acknowledge those who helped and inspired me in my entire life.

TABLE OF CONTENTS

Declaration i

Abstract ii

Dedication iii

Acknowledgments iv

Table of contents v

List of Figures vii

List of Tables ix

List of Abbreviations x

1. Introduction 1

1.1. Motivation 5

1.2. Contribution of the dissertation 5

1.3. Related work 6

2. Proposed M-D Multi-notch IIR filter 10

2.1. Notation 10

2.2. Filter structure 10

2.2.1. 1-D filter structure 10

2.2.2. 2-D filter structure 16

2.2.3. M-D filter structure 17

2.3. Implementation of the filter 17

3. Experimental results 18

3.1. 2-D notch filter 18

3.2. 3-D notch filter 23

3.3. Comparison with existing methods 26

4. Conclusion and Future work 31

4.1. Conclusions 31

4.2. Future work 31

References 33

LIST OF FIGURES

Figure 1.1: Segment of digitized human speech 1
Figure 1.2: A monochromatic image 1
Figure 1.3: fMRI image (Source - https://www.biopac.com/events/fmri-psych/) 2
Figure 1.4: 1-D single notch filter 3
Figure 1.5: Pole/Zero plot 3
Figure 1.6: Unfiltered and Filtered ECG Signal 4
Figure 1.7: Block diagram for 2-D IIR notch filter design by Pei *et al.* [19] 6
Figure 1.8: General feedback structure proposed in [21]. 7
Figure 1.9: Input and output image of the 2-D notch filter 8
Figure 1.10: 3-D notch filter 8
Figure 1.11: Structure of the 3-D notch filter [16] 9
Figure 2.1: 1-D notch filter structure 10
Figure 2.2: Pole/zero plot of first notch filter 11
Figure 2.3: Magnitude and phase response of first notch filter 12
Figure 2.4: Pole/zero plot of second notch filter 13
Figure 2.5: Magnitude and phase response of second notch filter 13
Figure 2.6: Pole/zero plot of combined notch filter 14
Figure 2.7: Magnitude and phase response of combined notch filter 15
Figure 2.8: Proposed 2-D notch filter 16
Figure 2.9: Proposed M-D notch filter 17
Figure 3.1: Magnitude response of proposed 2-D filter 18
Figure 3.2: Placement of the notches 19
Figure 3.3: Image of Lena Forsén (Source - https://en.wikipedia.org/wiki/Lenna) 20
Figure 3.4: Sinusoidal interference 20
Figure 3.5: Image with added interference 20
Figure 3.6: Output of $H_1(\boldsymbol{z})$ 22
Figure 3.7: Output of $H_2(\boldsymbol{z})$ 22
Figure 3.8: Output of $H_3(\boldsymbol{z})$ 22
Figure 3.9: Output of $H_4(\boldsymbol{z})$ 22
Figure 3.10: Output of $H_5(\boldsymbol{z})$ 22
Figure 3.11: Output of $H_6(\boldsymbol{z})$ 22
Figure 3.12: Image with padding 23
Figure 3.13: Un-padded image after filtering 23
Figure 3.14: -3dB iso surface of the notch locations 23
Figure 3.15: Magnitude response of 3-D notch filter 24
Figure 3.16: (a) 20^{th} frame of interference signal; (b) 178^{th} frame of interference signal 25

Figure 3.17: Unity 3-D image at 50th plane (n=50)..... 27
Figure 3.18: (a) Degraded Image; (b) Error Image; (c) Recovered image 29
Figure 3.19: SIR comparison 30

LIST OF TABLES

Table 3.1: Notch location details of 2-D filter 19
Table 3.2: Interference frequencies 21
Table 3.3: Notch details for 2-D notch filter 21
Table 3.4: Notch location details of 3-D filter 23
Table 3.5: Interference frequency details for video signal 24
Table 3.6: Notch filter details for video signal 25
Table 3.7: Attenuation of the inference of the video signal 25
Table 3.8: Notch details for unity 3-D degraded image 27
Table 3.9: Improved SIR of the proposed IIR notch filter 29

LIST OF ABBREVIATIONS

1-D	One-Dimensional
2-D	Two-Dimensional
3-D	Three-Dimensional
4-D	Four-Dimensional
5-D	Five-Dimensional
7-D	Seven-Dimensional
BIBO	Bounded-Input-Bounded-Output
DSP	Digital Signal Processing
ECG	Electrocardiography
FIR	Finite Impulse Response
fMRI	Functional Magnetic Resonance Imaging
IIR	Infinite Impulse Response
M-D	Multi-Dimensional
SIR	Signal-to-Interference Ratio

1. INTRODUCTION

Signals can be classified based on the number of independent variables. A signal that contains only one variable is said to be one-dimensional (1-D) signals [1]. Human voice is considered to be an example for a 1-D signal as the fluctuations of the air pressure as a function of time as illustrated in Figure 1.1. A monochromatic image is considered as a two-dimensional (2-D) signal, where the light intensity is represented as a function of horizontal and vertical displacement as shown in Figure 1.2.

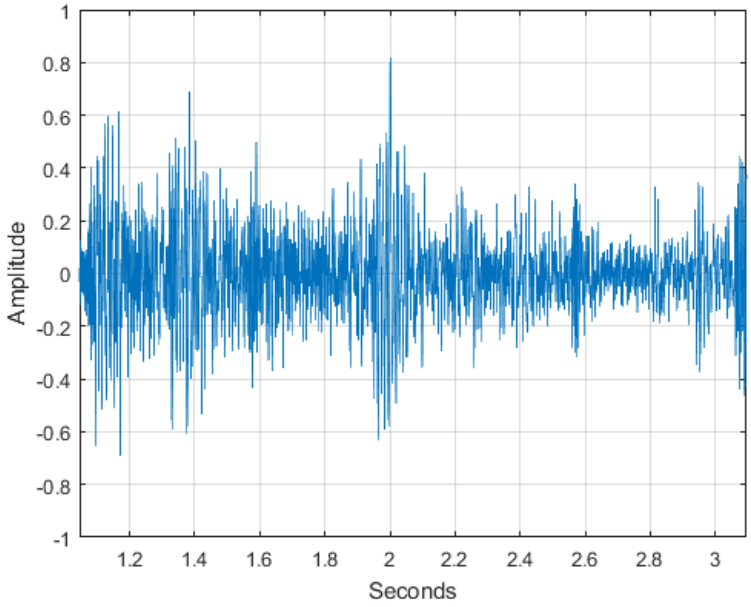

Figure 1.1: Segment of digitized human speech

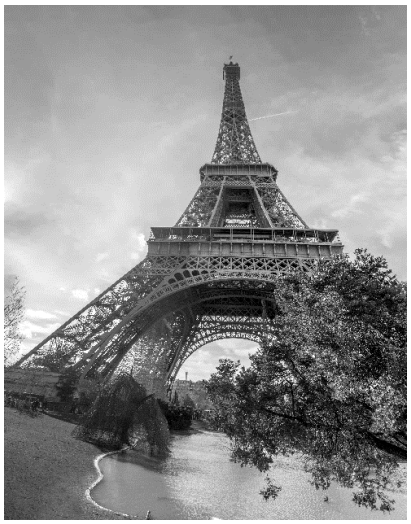

Figure 1.2: A monochromatic image

A Multi-dimensional (M-D) signal is a function of two or more than two independent variables. A video is considered as a three-dimensional (3-D) signal, as it is a function of three independent variables which are time and two spatial coordinates.

A human body is imaged as a group of cubes in functional magnetic resonance imaging (fMRI). Each cube is defined as voxel where it defines a point in 3-D space. A series of voxels are produced as a function of time [2]. Therefore, the output signal of the fMRI is defined as 4-D signal as shown in the Figure 1.3.

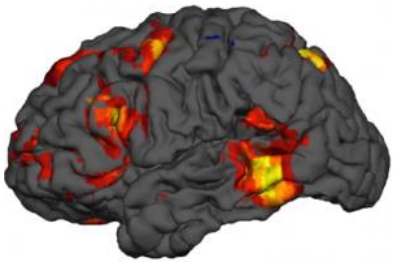

Figure 1.3: fMRI image (Source - https://www.biopac.com/events/fmri-psych/)

Light rays that are emanating from an object is defined by seven-dimensional (7-D) plenoptic function. It describes the intensity of the light rays passing through the center of an ideal camera. The 3-D space (x, y and z) location, every possible angles (θ, φ) [3], for every wave length and time is considered as seven dimensions [4]. 4-D light fields and five-dimensional (5-D) light field videos [5] are simplified version of 7-D plenoptic function [6].

Digital signal processing (DSP) technology and its advancements have dramatically impacted the modern society. The applications of DSP are impacted for many different fields. Without DSP, medical instruments would be less efficient. If there were no digital electrocardiography (ECG), or digital radiography and other medical imaging modalities it would be impossible to provide precise diagnoses. Digital/Internet audio or video, digital recording media such as CD, DVD, MP3 players, digital cameras, mobile phones, digital satellite and TV and wired/wireless networks are existing because of DSP technology.

Digital filters are a very important part of DSP. The main function of a filter is signal separation. It is needed for removing the interference from a signal. Among the different types of filters, notch filter has taken an important place as it is used to attenuate narrow band interfering signals. Notch filter is characterized by unit gain for all frequencies except at the notch where the gain is zero as shown in Figure 1.4. The zeros of the transfer function are

placed on the unit circle of the pole zero plot as shown in Figure 1.5. The shape of the notch is determined by the radius of the poles. The closer poles to the zeros, the sharper notch can be achieved.

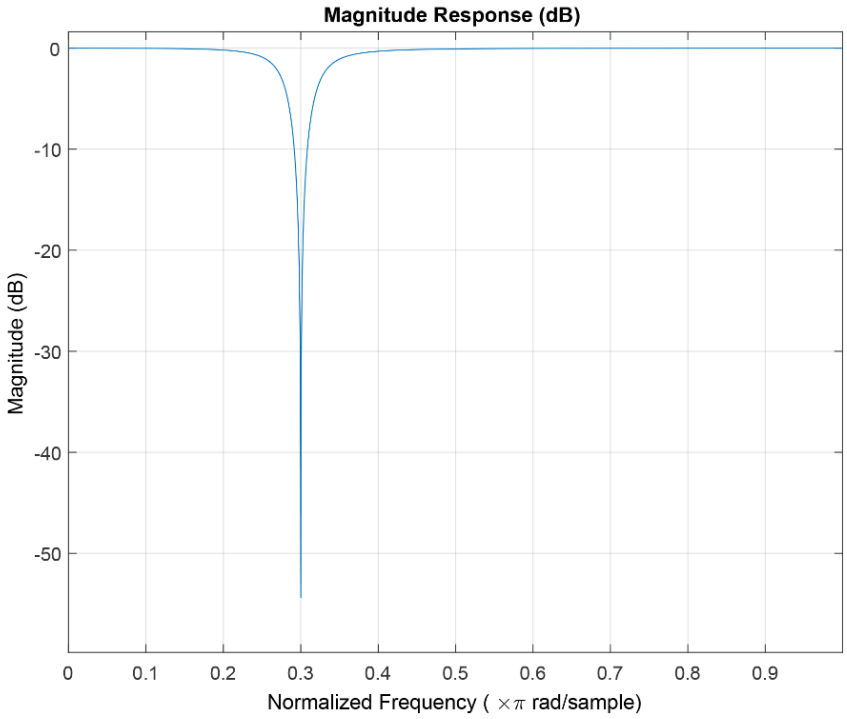

Figure 1.4: 1-D single notch filter

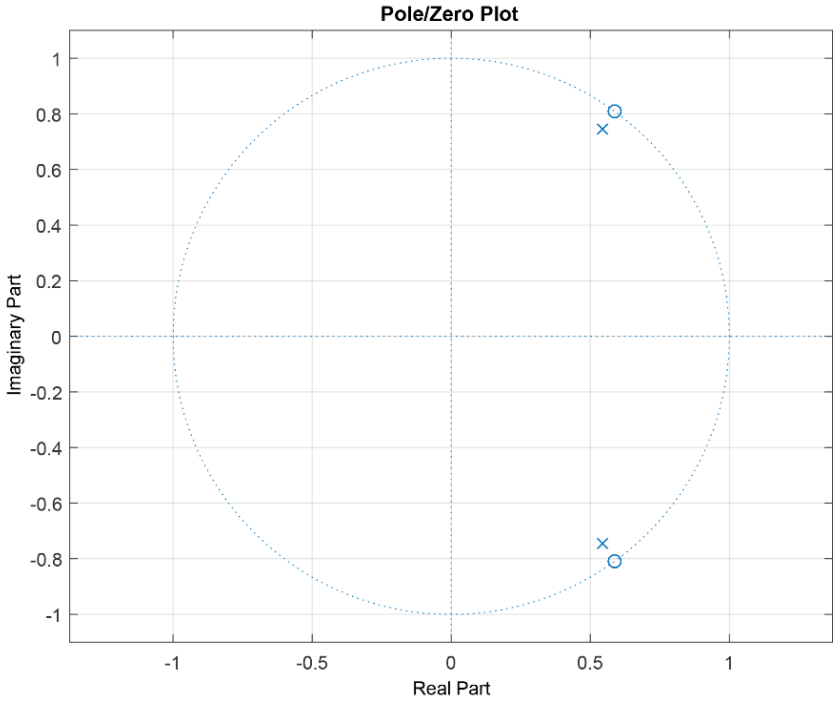

Figure 1.5: Pole/Zero plot

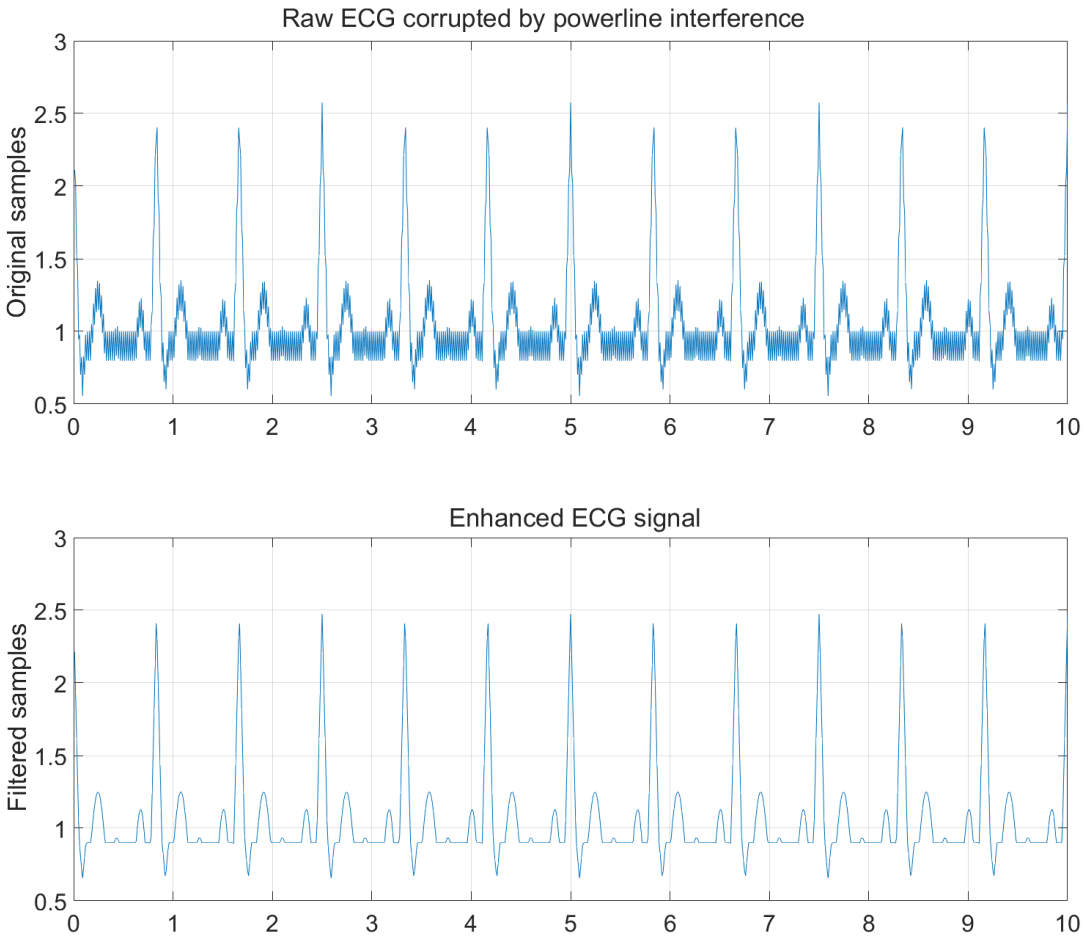

Figure 1.6: Unfiltered and Filtered ECG Signal

There are many applications that uses notch filters to remove the interference frequencies [7] [8]. Notch filters can be M-D as well as single or multiple notches.

The major application of notch filter is used to eliminate the narrow band interference in the area of communication [9] [10] [11], instrumentation, control and bio medical engineering. The captured electrocardiogram (ECG) signal is contaminated by strong disturbances such as power line interference, breathing artefacts and DC components. Notch filters can remove such unwanted signals before further processing. Raw and filtered ECGs are shown in Figure 1.6.

4-D light field/JPEG data is highly compressed and contains noticeable degradation due to blocking artifacts [12] [13] [14]. A gradient image has artificial edges due to blocking artifacts and can be reduced using a 2-D multiple notch filter [15].

1.1. Motivation

Removing interference components from 1-D and M-D signals are essential for further process the signals. There have been many studies carried out for the notch filters due to its usefulness. Multiple notches are achieved and named as a comb filter. The general comb filter consists of notches that are placed evenly. The introduced notch filters until now, is capable of processing only real-valued interfering signals. The motivation for this dissertation to introduce a general frame work for M-D, multi-notch filter to attenuate both real-valued and complex-valued narrowband interfering signals.

1.2. Contribution of the dissertation

In this dissertation, A generalised framework for the M-D IIR multi-notch filter is introduced. The multiple notches can be defined arbitrary and can be placed anywhere within the 1-D or M-D. The bandwidth of each notch can be changed independently. The related research papers have been studied to identify the existing filtering methods and future developments. Proposed notch filter is addressed to the limitations of the existing methods.

The proposed M-D IIR multi notch filter is implemented on software platform. Bandwidth for each notch can be defined separately to increase the flexibility of the filter. Experiments have been carried out for the monochromatic image, a grayscale video and a special unity 3-D image for comparison.

A comparison has been done to measure the effectiveness of the filtering capabilities of the proposed method. It clearly outperforms the existing M-D IIR notch filters compared to [16]. The signal-to-interference ratio (SIR) is much greater than the existing IIR notch filters.

M-D IIR multi-notch filter is required lower computational power to implement. It is vital to have a stable filter to achieve better filtering characteristics. The proposed generalised filter structure is always bounded-input-bounded-output (BIBO) stable.

1.3. Related work

Eliminate sinusoidal or narrow-band interference in digital signals while preserving the other frequency components intact is the primary objective of a notch filter [17]. There are two basic types of digital notch filters categorized as below.

- IIR filters
- FIR filters

IIR filters are potentially unstable and FIR filters are unconditionally stable because FIR filters contain only zeros where as IIR filters contain zeros and poles. An FIR filter needs higher filter orders than IIR filter for a given magnitude response [18]. This implies that IIR filters can be implemented with fewer adders and multipliers. By considering the above facts M-D IIR multi-notch filter is implemented and validated.

There are several studies carried out to design multiple notch filters. 2-D IIR filter design is proposed by Pei *et al.* in 1993 [19]. The IIR filter is implemented by cascading a parallel line filter and straight-line filter as shown in Figure 1.7.

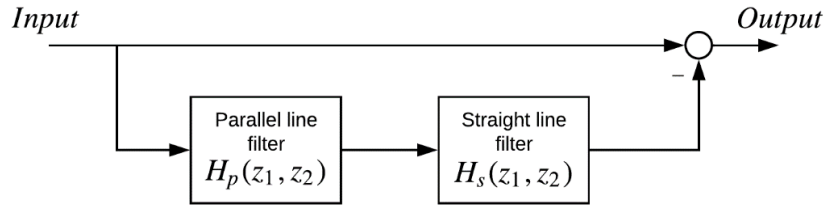

Figure 1.7: Block diagram for 2-D IIR notch filter design by Pei *et al.* [19]

The 2-D parallel line filter is designed by cascading two band pass filters and straight-line filter is derived from frequency transformation of 2-D analog prototype filter. The output of the IIR filter consists of two notches. It is noticed that by cascading parallel line filter and straight-line filter, even number of notches can be generated. There is no possibility of generating odd number of notches. Additionally, the generated two notches always at the second quadrant. The input signal is always reoriented in to the second quadrant for filtration thus the flexibility filter is limited.

Pei *et al.* introduced another 2-D IIR notch filter design using outer product expansion [20]. Two 1-D notch filters are cascaded to generate the magnitude response of 2-D notch filter. The advantage of proposed method is having a smaller number of multiplications than previously introduced methods. A single sinusoidal interference is added to an image. Two

notches are implemented to remove both real positive and negative frequency components. The proposed notch filter is tested only for two notches and has less flexibility for expanding.

Ideal notch filter has unit gain in all other frequencies other than notch frequency and the 3dB bandwidth is a small value. In a practical filter there will be some transients and the 3dB bandwidth will be a positive value. Pei *et al*. introduced a general feedback structure to have a narrower stopband for 1-D and 2-D notch filters [21].

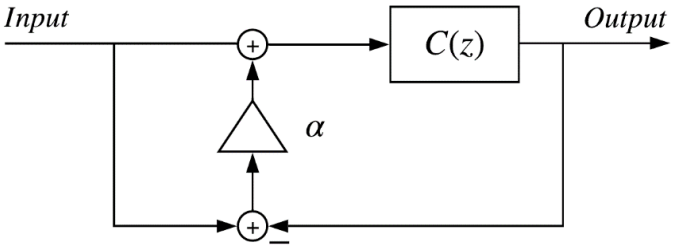

Figure 1.8: General feedback structure proposed in [21].

$C(z)$ is considered as any type of notch filter as shown in Figure 1.8. The transfer function of the proposed feedback structure is given by

$$H(z) = \frac{(1+\alpha)C(z)}{1+\alpha C(z)}, \tag{1}$$

where $\alpha \geq 0$ for stability.

The ideal magnitude response for 1-D notch filter is as below.

$$A(\omega) = \begin{cases} 0, & \omega = \omega^* \\ 1, & otherwise \end{cases} \tag{2}$$

where ω^* represents the notch frequency. The simplest conventional IIR notch filter is given by,

$$C(z) = \frac{1 - 2\cos(\omega^*)z^{-1} + z^{-2}}{1 - 2\rho\cos(\omega^*)z^{-1} + \rho^2 z^{-2}} = \frac{N(z)}{D(z)}, \tag{3}$$

where ρ is the pole's radius of $C(z)$ and is limited to $0 \leq \rho < 1$ for stability.

Figure 1.9: Input and output image of the 2-D notch filter

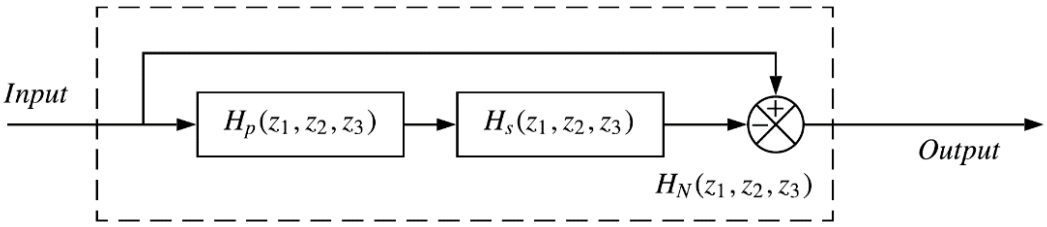

Figure 1.10: 3-D notch filter

The performance of the conventional filter is improved by implementing the feedback method and it has less 3dB bandwidth than conventional method. The latter part of this research, by combining two 1-D notch filters, a 2-D notch filter is implemented as single notch pair. The implemented method is tested by removing a sinusoidal interference from a monochromatic image as shown in Figure 1.9.

The interference of the image has been removed by the filter drastically. However, there are some interference components exist in the output image. This method can only introduce notches as pairs.

Ahmed Chinoun *et al*., in 2019 introduced 3-D IIR notch filter consists of all-pass filter and straight-line filter based on lattice structure [22]. The proposed filter structure is illustrated in Figure 1.10. H_p and H_s denote the all-pass filter and straight-line filter respectively. The proposed 3-D notch filter does not contain any iterative methods or optimisation. Therefore, exact frequency will not be supressed using this method as the stop band ripple is high.

Non-separable 3-D IIR notch filter design is introduced using outer product expansion by Piyachaiyakul *et al*. [16]. Figure 1.11 illustrates the block diagram of the 3-D IIR notch filter. The filter design is divided into three processes such as 2-D IIR notch filter design, 1- D IIR notch filter design and combination between 1-D and 2-D notch filters.

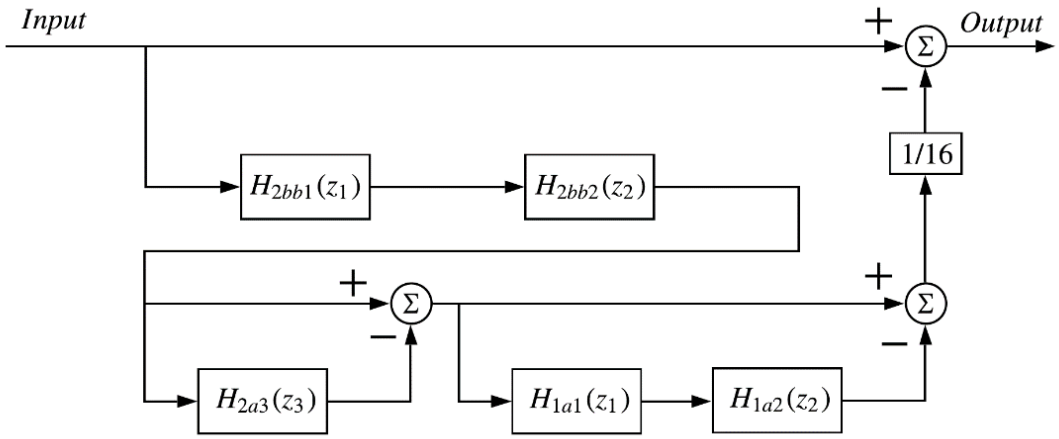

Figure 1.11: Structure of the 3-D notch filter [16]

The first subscript of the filter transfer function denotes the order of the filter, whereas the number at the end of subscript expresses the dimension of the filter. H_{1a2} means the first order all-pass filter of the second dimension and H_{2bb1}, H_{2bb2} are second order 1-D bandpass filter of the first and second dimensions respectively. A simulation has been done to measure the effectiveness of the interference removal. A unity 3-D image has been used as an input to the proposed filter. The effectiveness of the filter is measured by evaluating the SIR values before and after filtering.

2. PROPOSED M-D MULTI-NOTCH IIR FILTER

The design of the proposed M-D multi-notch IIR filter is described in detail in this chapter. 1-D, 2-D filter structures are explained and M-D filter structure is derived. The introduced generalised framework has the flexibility of adding any number of notches and can be controlled the locations, shape of the notch independently.

2.1. Notation

The following notation scheme is employed in this dissertation. The frequency response of the M-D multi-notch filter containing N notches.

$$H\left(e^{j\omega_1}, e^{j\omega_2}, \dots, e^{j\omega_n}\right) = \begin{cases} 0, & \omega = \omega^* \\ 1, & Otherwise \end{cases} \quad (4)$$

where $(\omega_1^*, \omega_2^*, \dots, \omega_n^*)$ are the notch frequencies inside the principal Nyquist hypercube.

2.2. Filter structure

Initially, 1-D filter structure is presented and afterwards it will be expanded as an M-D filter. The 1-D multi- notch IIR filter structure is illustrated in Figure 2.1. Each notch filter block is connected in cascade. There are m blocks for 1-D case that represent m number of notches. Each one will remove a particular frequency.

2.2.1. 1-D filter structure

The proposed notch filter structure for 1-D is illustrated in Figure 2.1. Each filter block consists of two notch filters as $H(\boldsymbol{z})$ and $H(\boldsymbol{z^{-1}})$.

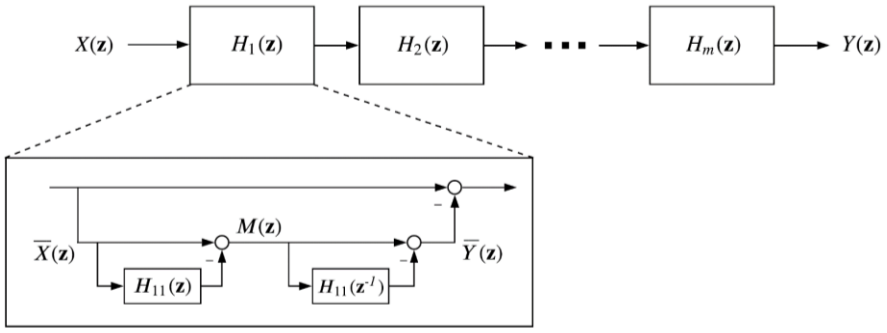

Figure 2.1: 1-D notch filter structure

$$\bar{Y}(\boldsymbol{z}) = M(\boldsymbol{z})\left(1 - H_{11}(\boldsymbol{z^{-1}})\right) \tag{5}$$

$$M(\boldsymbol{z}) = \bar{X}(\boldsymbol{z})\left(1 - H_{11}(\boldsymbol{z})\right) \tag{6}$$

From (5) and (6),

$$\frac{\bar{Y}(\boldsymbol{z})}{\bar{X}(\boldsymbol{z})} = \left(1 - H_{11}(\boldsymbol{z})\right)\left(1 - H_{11}(\boldsymbol{z^{-1}})\right) = G(\boldsymbol{z})G(1/\boldsymbol{z}) \tag{7}$$

The first notch filter $H_{11}(z)$ is defined as below [23].

$$H_{11}(\boldsymbol{z}) = \frac{\left[z - e^{j\omega_0}\right]}{\left[z - re^{j\omega_0}\right]}, \tag{8}$$

where -$\pi \leq \omega_0 \leq \pi$ and $|r| \leq 1$ are cut-off frequency and pole radius. The equivalent transfer function can be written as below.

$$G(\boldsymbol{z}) = 1 - H_{11}(\boldsymbol{z}) = \frac{\left[(1-r)e^{j\omega_0}\right]}{\left[z - re^{j\omega_0}\right]} \tag{9}$$

It contains a pole in the z-plane and is illustrated in Figure 2.2. Magnitude and phase response are illustrated in Figure 2.3. When r is closer to 1, a sharper notch can be achieved. $H(z)$ filter is causal and stable since the pole is inside the unit circle.

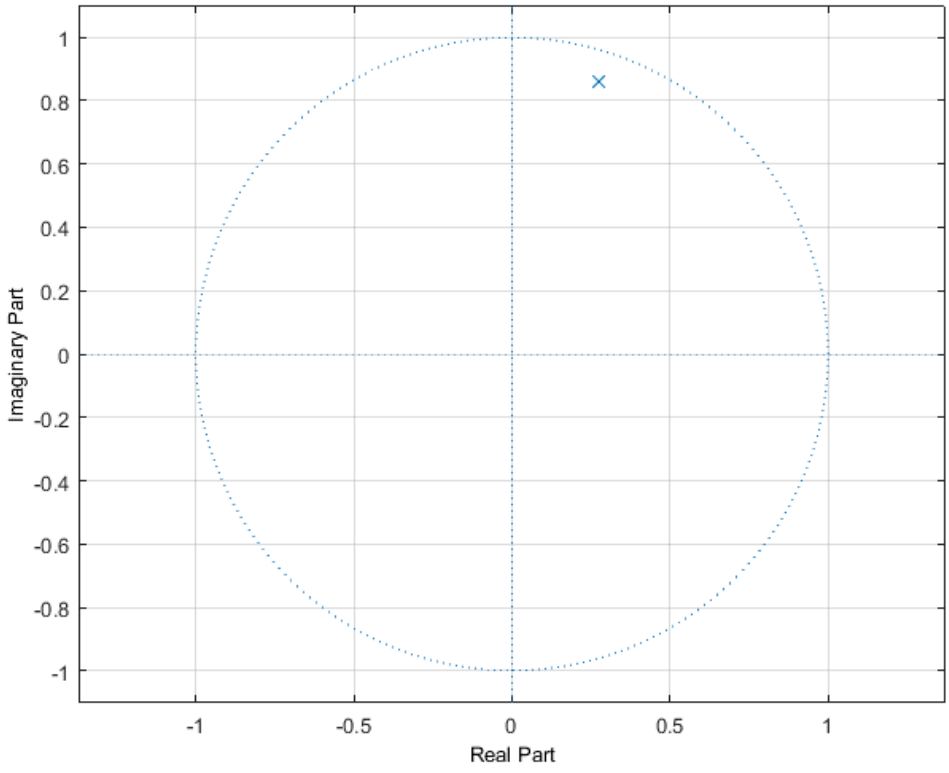

Figure 2.2: Pole/zero plot of first notch filter

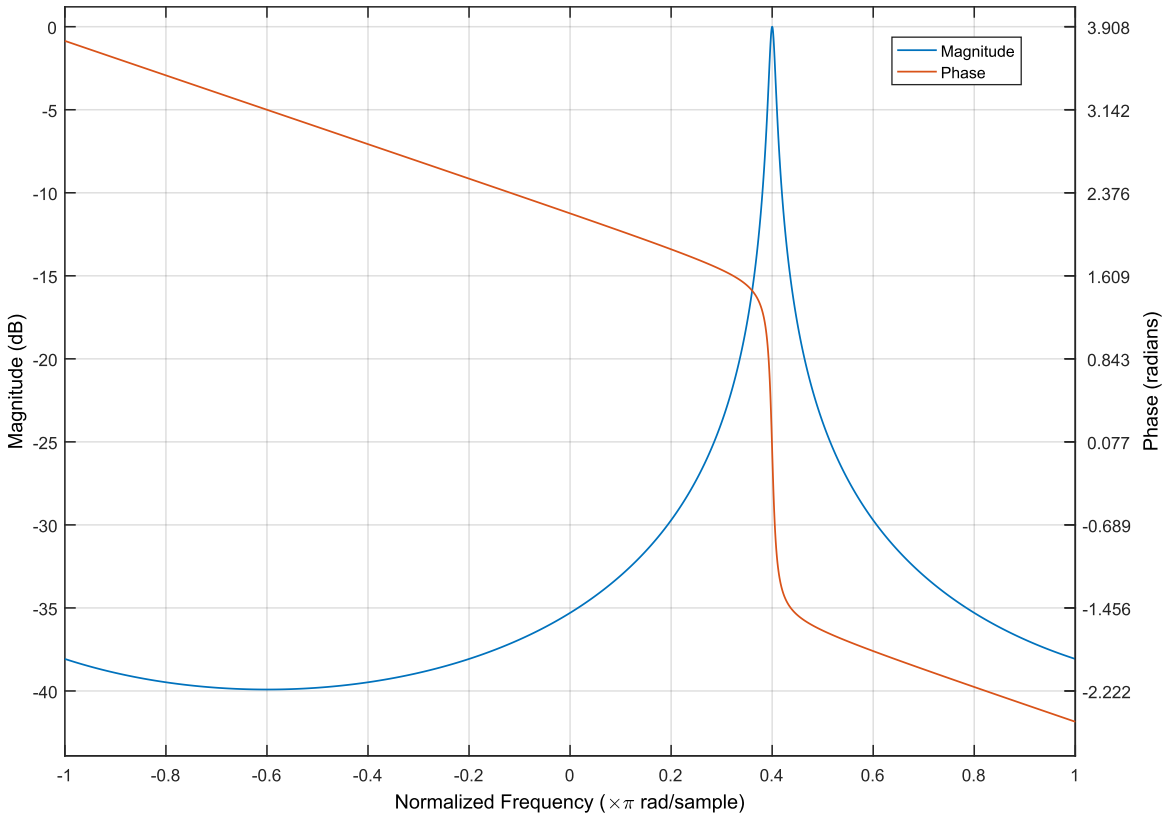

Figure 2.3: Magnitude and phase response of first notch filter

The second notch filter is defined in (10) and (11).

$$H_{11}(z^{-1}) = \frac{[z - e^{j\omega_0}]}{[zr - e^{j\omega_0}]} \tag{10}$$

$$G(1/\boldsymbol{z}) = 1 - H(z^{-1}) = \frac{[(r-1)z]}{[zr - e^{j\omega_0}]} \tag{11}$$

The second notch filter contains a pole that is outside of the unit circle and a zero that is on the center of the unit circle.

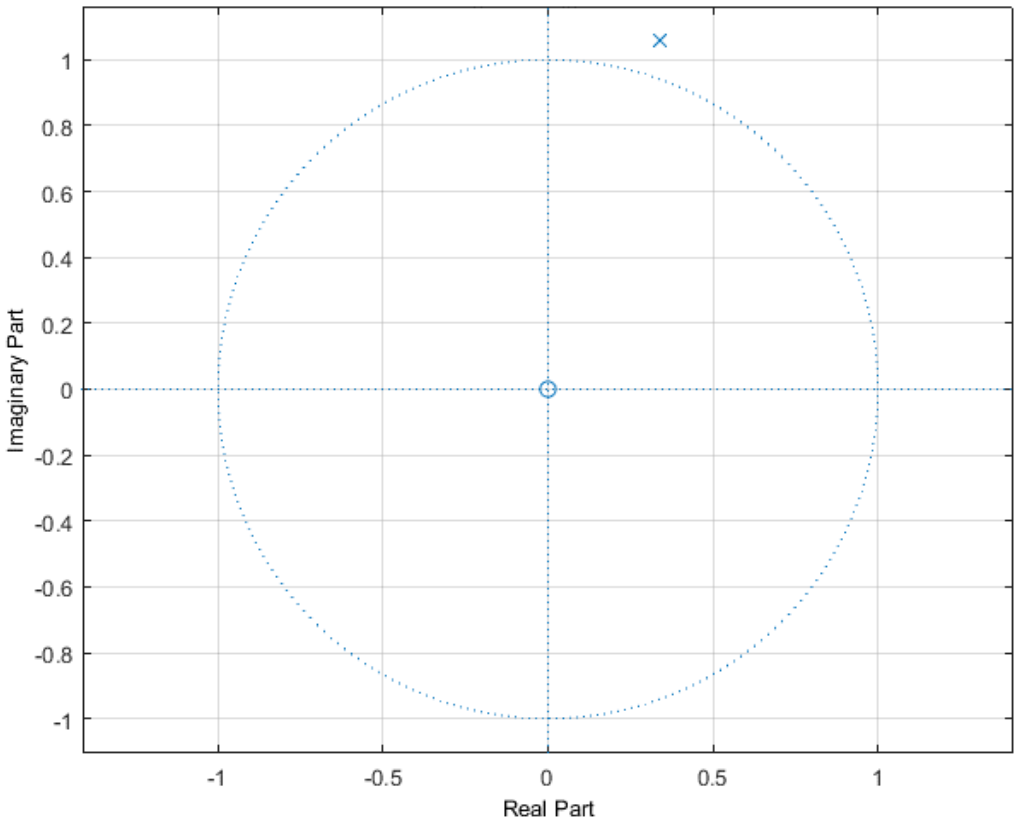

Figure 2.4: Pole/zero plot of second notch filter

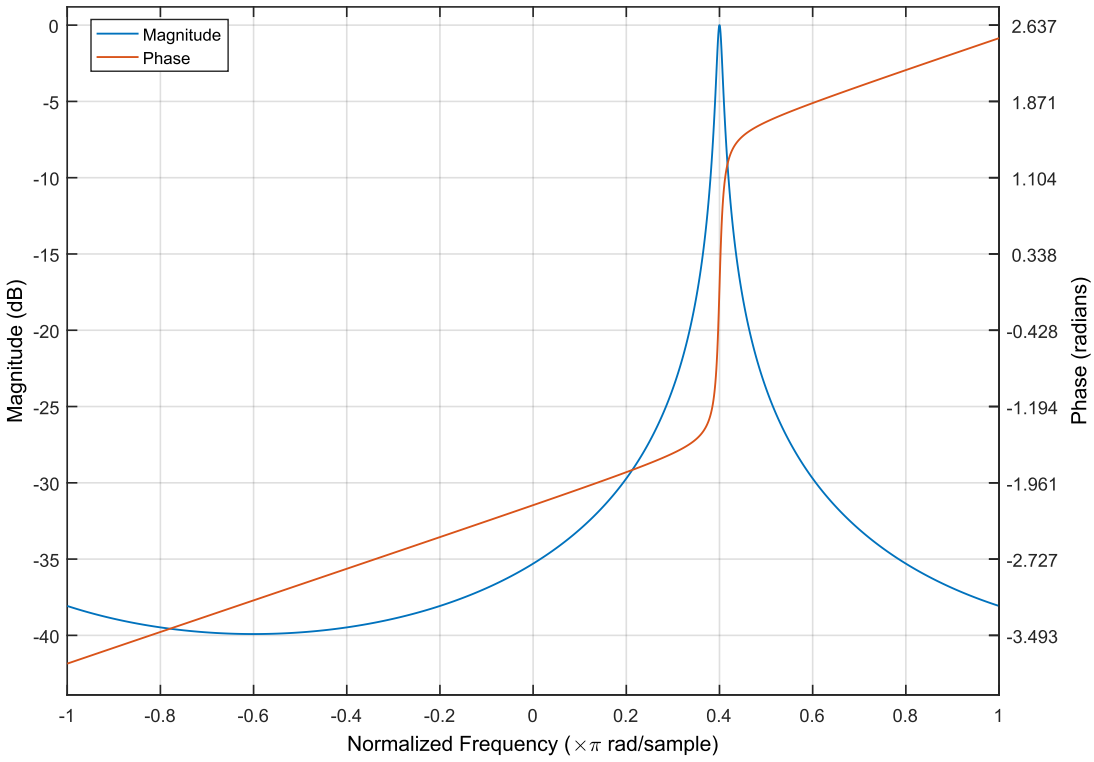

Figure 2.5: Magnitude and phase response of second notch filter

Figure 2.4 and Figure 2.5 are illustrated the pole/zero plot, magnitude and phase response of the second notch filter respectively. The magnitude response is similar in both notch filters. $H_{11}(z^{-1})$ is anti-causal and the pole is at the outside of the unit circle. It will be used as revered direction thus the filter is stable. There is a non-zero phase response in both notch filters and mirrored along the vertical axis. Once the two filters are combined together, zero phase filtering can be achieved as shown in the Figure 2.6 and Figure 2.7. The transfer function of the combined notch filter is defined in (12).

$$H_1(z) = 1 - \frac{\left[\left((1-r)e^{j\omega_0}\right)(r-1)z\right]}{(z - re^{j\omega_0})(zr - e^{j\omega_0})} \tag{12}$$

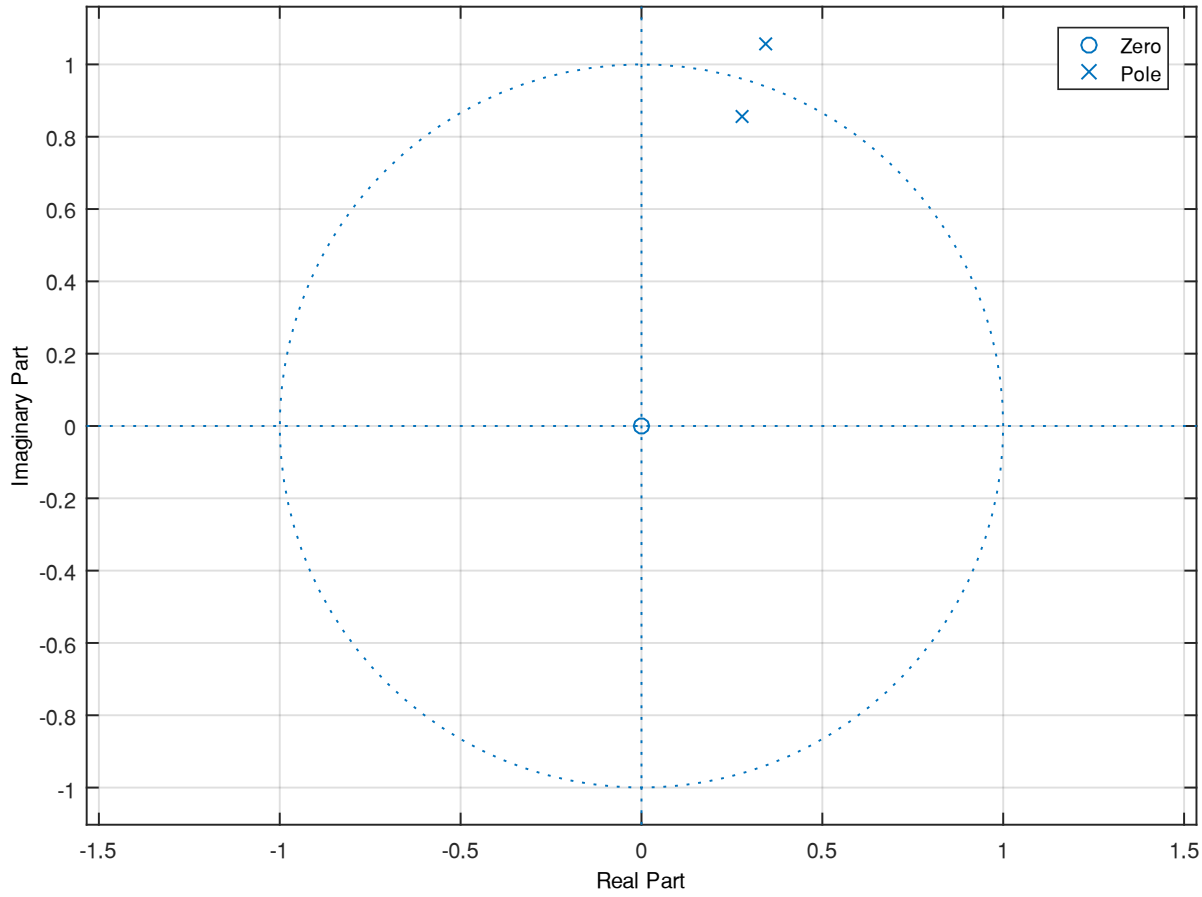

Figure 2.6: Pole/zero plot of combined notch filter

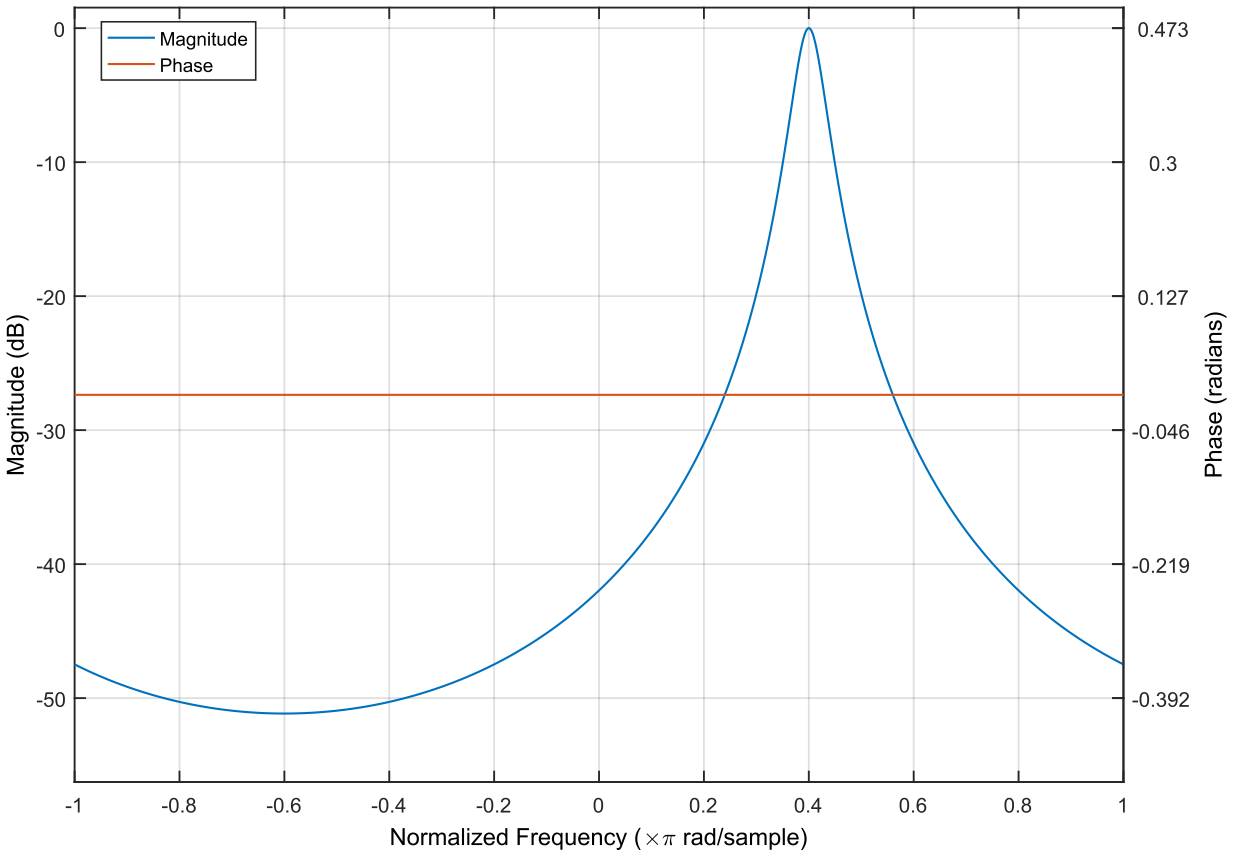

Figure 2.7: Magnitude and phase response of combined notch filter

2.2.2. 2-D filter structure

The proposed method for 1-D notch filter is extended for 2-D notch filter. Each filter block consists of four filters and connected serially as demonstrated in Figure 2.8. There are m number of notches can be defined using $H_1(\boldsymbol{z})$ to $H_m(\boldsymbol{z})$ filter blocks. $H_1(\boldsymbol{z})$ consists of four filters named as $H_{11}(z)$, $H_{11}(z^{-1})$, $H_{12}(z)$ and $H_{12}(z^{-1})$. First pair of filters correspond to a single notch in one dimension. For an example If the input signal is 2-D and consisting of three frequencies to be attenuated, three notches have to be implemented. Therefore, twelve filters are needed to need to supress the all three interference frequencies in the 2-D signal.

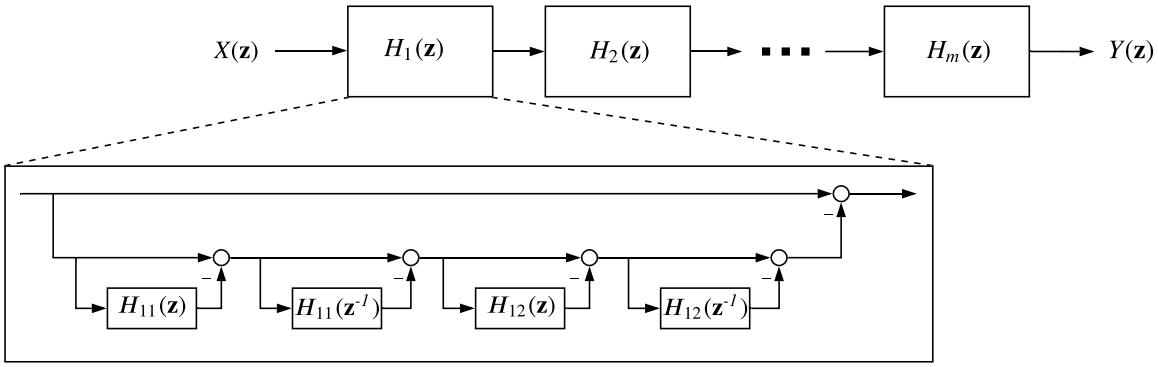

Figure 2.8: Proposed 2-D notch filter

Transfer function for the $H_1(z)$ is derived using the 1-D notch filter.

$$H_1(z) = 1 - \frac{\left[\left((1-r_1)e^{j\omega_0}\right)(r_1-1)z\right]\left[\left((1-r_2)e^{j\omega_1}\right)(r_2-1)z\right]}{\left[(z-r_1e^{j\omega_0})(zr_1-e^{j\omega_0})\right]\left[(z-r_2e^{j\omega_1})(zr_2-e^{j\omega_1})\right]}\ , \qquad (13)$$

where -$\pi \leq \omega_0, \omega_1 \leq \pi$ and $|r_1|, |r_2| \leq 1$ are cut-off frequency and pole radius, respectively. The location of the 2-D notch is defined by ω_0 and ω_1 and the shape of the notch can be changed using r_1 and r_2. If r_1 and r_2 equal, the shape of the notch is symmetric. The proposed 2-D notch filter is extendable to any number of notches as well as can be placed any quadrant.

2.2.3. M-D filter structure

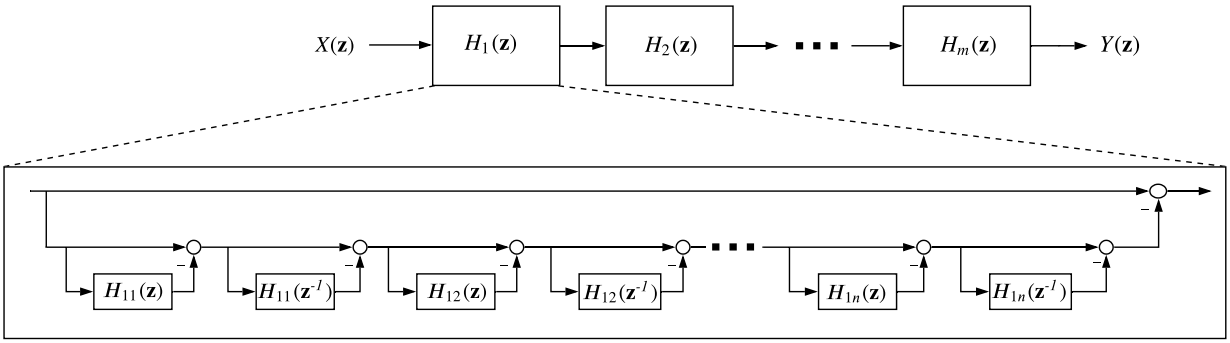

Figure 2.9: Proposed M-D notch filter

The proposed general framework is extended for designing the M-D notch filter as illustrated in Figure 2.9. $H_1(\boldsymbol{z})$ consists of n number of filter pairs corresponds to the dimensions of the input signal. m number of filter blocks can be defined depends on the number of interference frequencies. The locations and the number of notches can be placed without any limitations. Transfer function for the $H_1(z)$ is

$$H_1(z) = 1 - \frac{\left[\left((1-r_1)e^{j\omega_0}\right)(r_1-1)z\right]\left[\left((1-r_2)e^{j\omega_1}\right)(r_2-1)z\right]\ldots\left[\left((1-r_n)e^{j\omega_{n-1}}\right)(r_n-1)z\right]}{\left[(z-r_1e^{j\omega_0})(zr_1-e^{j\omega_0})\right]\left[(z-r_2e^{j\omega_1})(zr_2-e^{j\omega_1})\right]\ldots\left[(z-r_ne^{j\omega_{n-1}})(zr_n-e^{j\omega_{n-1}})\right]}\ , \qquad (14)$$

where -$\pi \leq \omega_0, \omega_1 \ldots \omega_{n-1} \leq \pi$ and $|r_1|, |r_2| \ldots |r_n| \leq 1$ are cut-off frequency and pole radius, respectively.

2.3. Implementation of the filter

Interference can have real as well as complex components. There are positive and negative frequencies can be identified, as the Fourier spectrum is symmetrical. Two conjugate notches are needed to eliminate interference if it has only the real components.

The introduced M-D multi-notch IIR filter has zero phase filtering characteristics. It is implemented by forward and backward filtering of the input signal. For backward filtering, entire or block of the input signal must be time-reversed. This creates a time delay for the filtering procedure. Therefore, this is can be applied directly to offline applications as the filter needs future sample values. However, this can be applied to real time applications with a sufficient delay time or block-wise filtering.

3. EXPERIMENTAL RESULTS

In this chapter, frequency response of the proposed 2-D and 3-D filter is derived. A monochromatic image is used as a 2-D input signal to the notch filter and results were reviewed after each filtering stage. Gray scale video is filtered using the proposed notch filter and few frames of the video is presented to represent the filtering capabilities across 3rd dimension. Finally, filtering characteristics were compared with existing method to prove the effectiveness of the M-D multi – notch IIR filter.

3.1. 2-D notch filter

The frequency response of the proposed 2-D filter is illustrated in Figure 3.1. Notches can be arbitrary placed and number of notches can be even or odd.

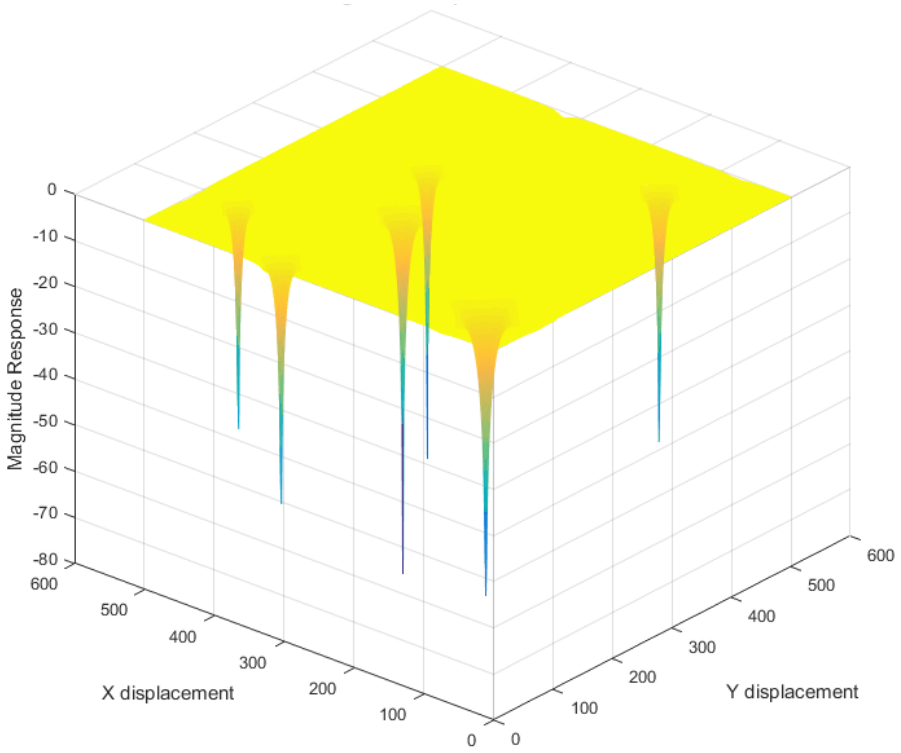

Figure 3.1: Magnitude response of proposed 2-D filter

The input variables for the notch filter are radius and angle of the pole. The pole angle is varying from $-\pi$ to π. The pole radius varies from 0 to 1. The location of each notch is determined by the value of the pole angle. For an example 500 x 500 grid has been taken into 2-D notch creation. Notch locations related to the magnitude response is shown in Table 3.1. Figure 3.2 is illustrate the locations of the notches of the magnitude response of the 2-D filter.

Table 3.1: Notch location details of 2-D filter

θ_1	r_1	θ_2	r_2
0.2π	0.9	0.4π	0.9
-0.2π	0.85	0.2π	0.85
-0.6π	0.9	0.8π	0.9
0.7π	0.88	-0.5π	0.88
-0.9π	0.88	0.3π	0.88
-0.7π	0.8	-0.7π	0.8

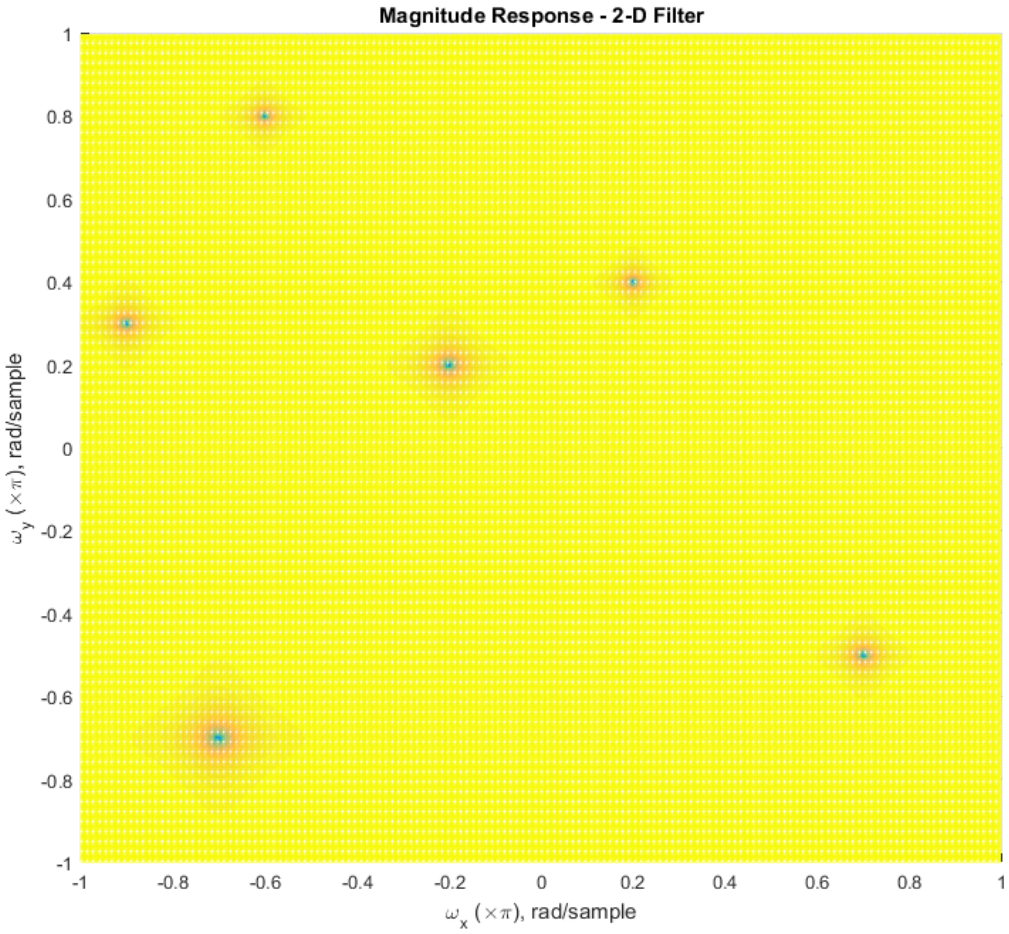

Figure 3.2: Placement of the notches

A monochromatic version of Lenna image is used as an input to the 2-D notch filter and illustrated in Figure 3.3. The original image is in RGB and size is 512 x 512 pixels.

Figure 3.3: Image of Lena Forsén (Source - https://en.wikipedia.org/wiki/Lenna)

A real sinusoidal interference has been added to the image as

$$I(n_1, n_2) = A \sin(\omega_1 n_1 + \omega_2 n_2 + \emptyset), \tag{15}$$

where ω_1, ω_2 and $\emptyset$ are interference frequencies and phase angle on the interference signal.

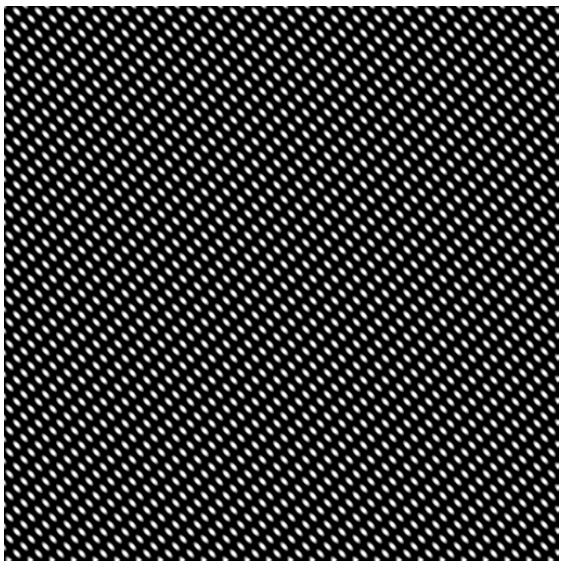

Figure 3.4: Sinusoidal interference

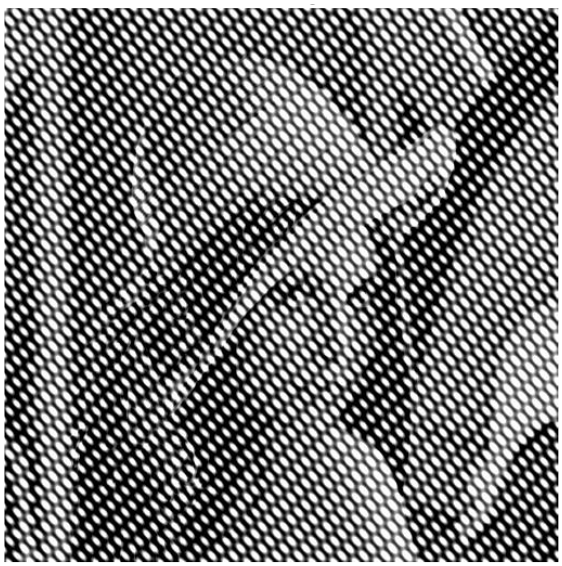

Figure 3.5: Image with added interference

Table 3.2: Interference frequencies

A	ω_1	ω_2	ϕ
0.3	0.1π	0.1π	0.5π
0.4	-0.2π	0.1π	0.5π
0.5	0.1π	-0.2π	0.5π

The interference component consists of three real sinusoidal components as illustrated in Table 3.2. The generated interference and the image with added interference are shown in Figure 3.4 and Figure 3.5 respectively. The notch locations and pole radius for the 2-D notch filter is illustrated in Table 3.3.

Table 3.3: Notch details for 2-D notch filter

θ_1	r_1	θ_2	r_2
0.1π	0.95	0.1π	0.95
-0.1π	0.95	-0.1π	0.95
-0.2π	0.95	0.1π	0.95
0.2π	0.95	-0.1π	0.95
0.1π	0.95	-0.2π	0.95
-0.1π	0.95	0.2π	0.95

Figure 3.5 consists of three interference frequencies. However, six filter blocks ($H_1(\boldsymbol{z})$ to $H_6(\boldsymbol{z})$) are needed in order to remove positive and negative frequencies. If the interference consists of real and complex components, only three filter blocks are needed. Figure 3.6, Figure 3.7, Figure 3.8, Figure 3.9, Figure 3.10 and Figure 3.11 illustrate the output image after each filtering blocks. The interference components have been removed in the output image after the 6^{th} filtering block. However, there is a transient at each filtering stage and interference remain around the boarder. In order to get rid of this artifact, a padding is introduced before the filtering stage. The amount of padding is depending on the amount of transient. Padding can be inserted as zeros or replica of the pixels at the border. Figure 3.12 and Figure 3.13 illustrate the final image after filtering and un-padded image respectively. The output image has same phase angle as input signal due to the zero phase characteristics. However, it will not be affected to the output signal due to the attenuated magnitude.

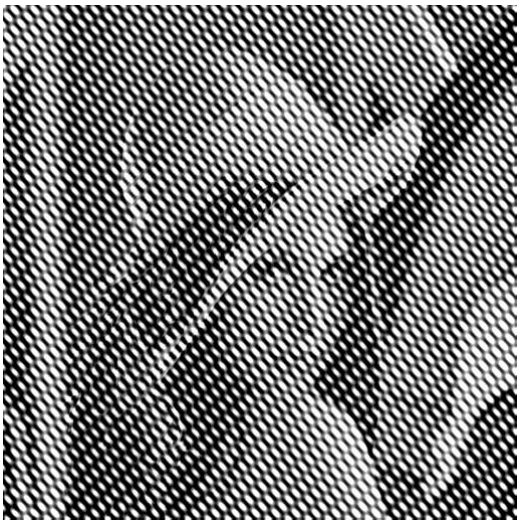

Figure 3.6: Output of $H_1(\boldsymbol{z})$

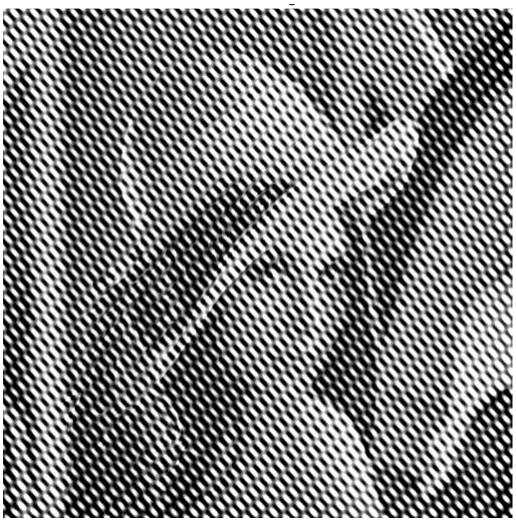

Figure 3.7: Output of $H_2(\boldsymbol{z})$

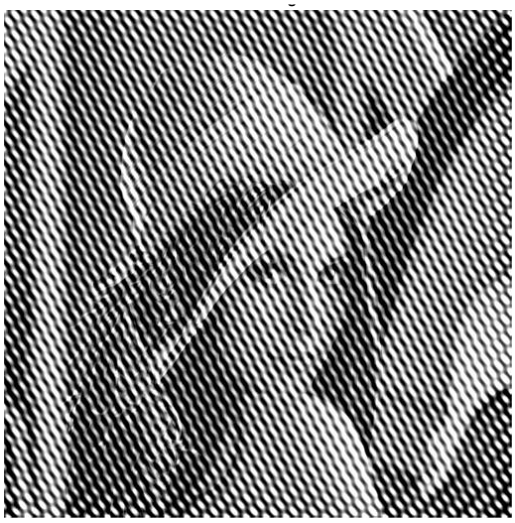

Figure 3.8: Output of $H_3(\boldsymbol{z})$

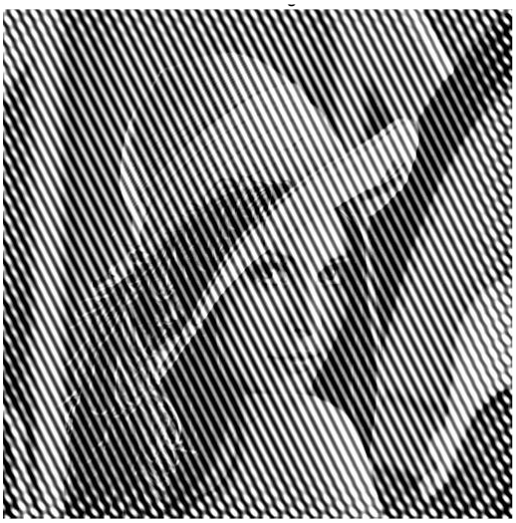

Figure 3.9: Output of $H_4(\boldsymbol{z})$

Figure 3.10: Output of $H_5(\boldsymbol{z})$

Figure 3.11: Output of $H_6(\boldsymbol{z})$

Figure 3.12: Image with padding

Figure 3.13: Un-padded image after filtering

3.2. 3-D notch filter

Figure 3.14 illustrates the location of each notch in 3-D space and iso surface for the -3dB bandwidth.

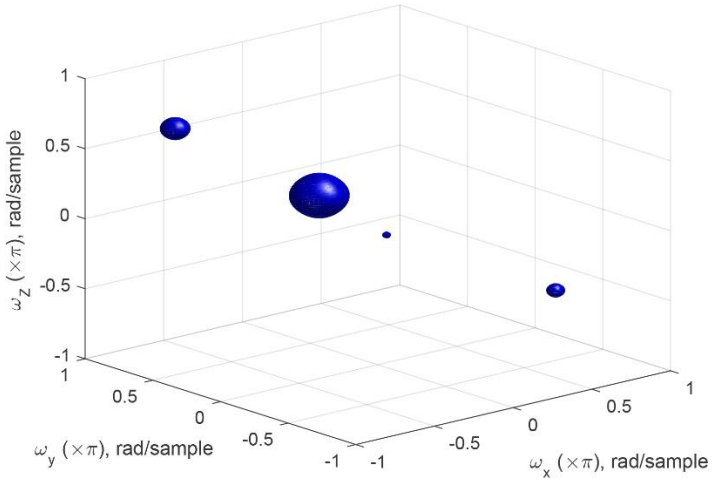

Figure 3.14: -3dB iso surface of the notch locations

Table 3.4: Notch location details of 3-D filter

θ_1	r_1	θ_2	r_2	θ_3	r_3
0.4π	0.9	0.4π	0.9	-0.3π	0.9
0.2π	0.5	-0.2π	0.5	0.2π	0.5
0.8π	0.7	-0.6π	0.7	0.6π	0.7
-0.5π	0.8	0.7π	0.8	-0.5π	0.8

The magnitude response can be plotted by for each ω_3 value. For an example first row of the Table 3.4 is shown in the Figure 3.15.

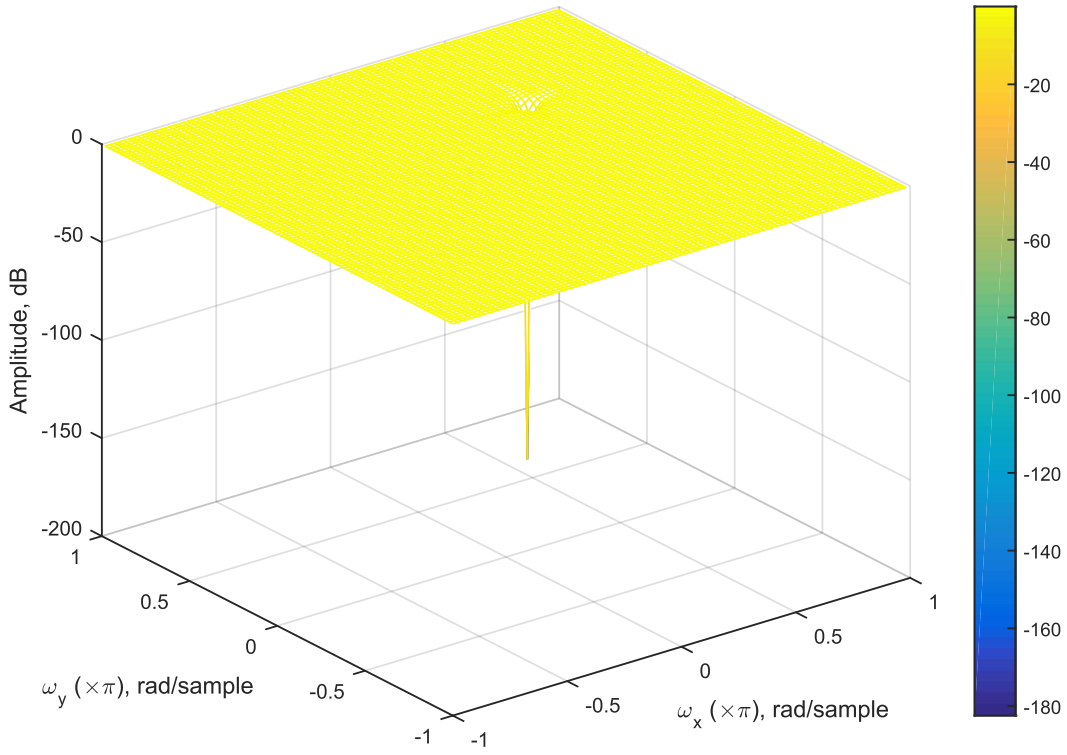

Figure 3.15: Magnitude response of 3-D notch filter

The M-D filter has been tested for a video signal as well. The height, width and number of frames are 426, 240 pixels and 350 respectively. A real sinusoidal interference has been added to the video signal as per the equation (2).

$$I(n_1, n_2, n_3) = A\sin(\omega_1 n_1 + \omega_2 n_2 + \omega_3 n_3) \tag{16}$$

Two interference elements have been added to the video as shown in the Table 3.5. Real sinusoidal interference is varying in all three dimensions. Figure 3.16 illustrates the 20th and 178th frame of the interference signal.

Table 3.5: Interference frequency details for video signal

A	ω_1	ω_2	ω_3
0.3	0.2π	0.1π	0.4π
0.3	-0.3π	0.2π	0.4π

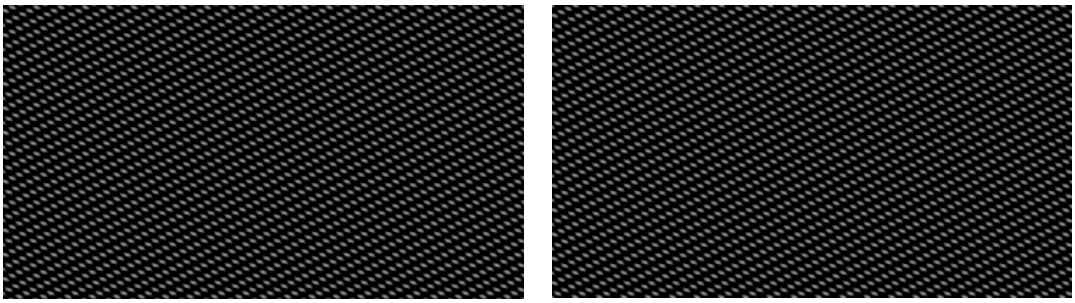

(a) (b)

Figure 3.16: (a) 20th frame of interference signal; (b) 178th frame of interference signal

The noisy video signal has been filtered in four filter blocks as per the M-D filter structure. The notch locations and respective pole radius for the 3-D notch filter as specified in the Table 3.6.

Table 3.6: Notch filter details for video signal

θ_1	r_1	θ_2	r_2	θ_3	r_3
0.2π	0.95	0.1π	0.95	0.4π	0.95
-0.2π	0.95	-0.1π	0.95	-0.4π	0.95
-0.3π	0.95	0.2π	0.95	0.4π	0.95
0.3π	0.95	-0.2π	0.95	-0.4π	0.95

The filtered video signal is shown in Table 3.7. The transient is present at each dimension. A padding is introduced to remove the transient artifact. The amount of padding is depending on the transient. It can be insert as zeros or replica of the pixels at each frame of the video signal.

Table 3.7: Attenuation of the inference of the video signal

Frame	Video signal with interference	Filtered video signal
20th	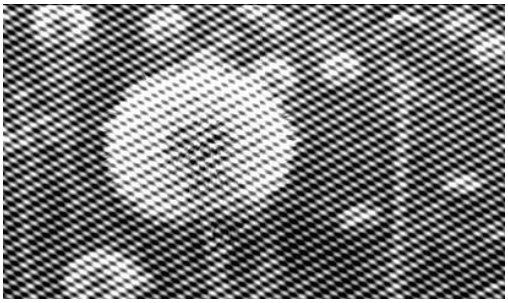 (a)	(b)

178th	(c)	(d)
334th	(e)	(f)

3.3. Comparison with existing methods

Piyachaiyakul *et al.* has been introduced 3-D IIR notch filter design using outer product expansion [16] . Special input called unity 3-D signal is used to measure the effectiveness of the filter. Figure 3.17 illustrates the unity 3-D image and defined as below.

$$v(l,m,n) = \begin{cases} 1, & 26 \le l \le 75, 26 \le m \le 75, 26 \le n \le 75 \\ 0, & Otherwise \end{cases}$$

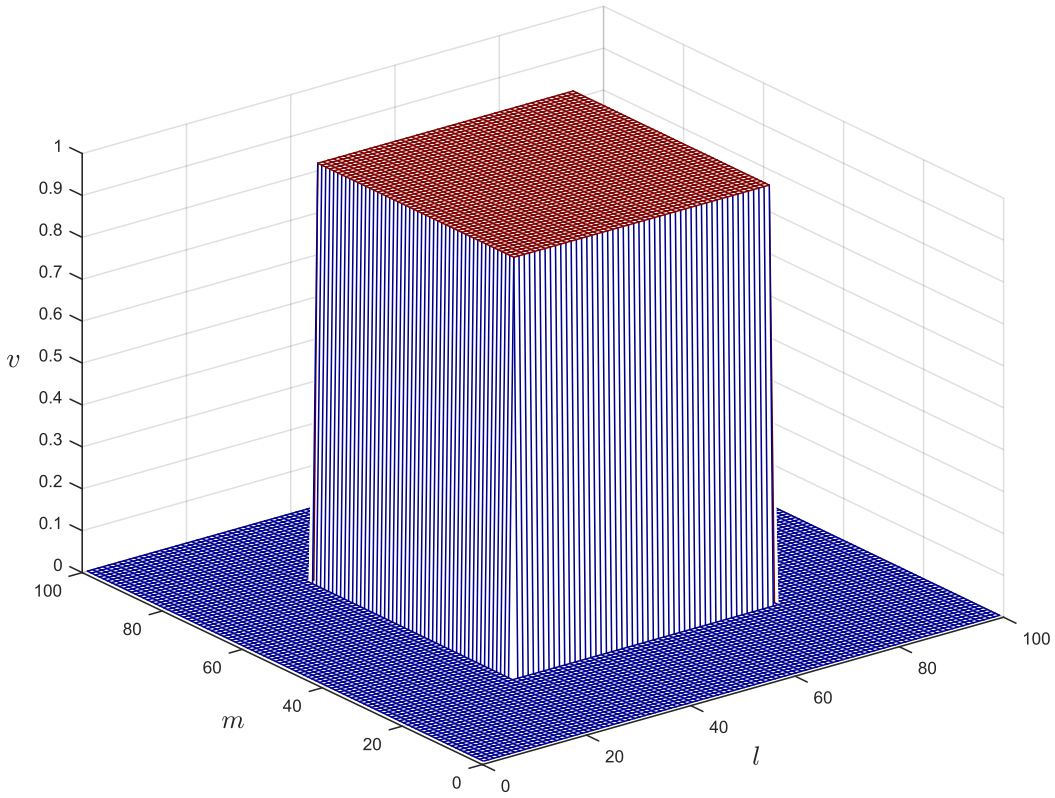

Figure 3.17: Unity 3-D image at 50th plane (n=50)

The comparison study has been done with Piyachaiyakul's method in order to measure the effectiveness of the proposed M-D multi-notch IIR filter. The same input signal is used in this study to compare the filtering characteristics. An interference component is added to the input signal as defined in equation (3).

$$x(l,m,n) = A\sin(\omega_1 l + \omega_2 m + \omega_3 n) \qquad (17)$$

Where, $\omega_1 = 0.2\pi,\ \omega_2 = 0.4\pi$ and $\omega_3 = 0.6\pi$. There is no complex component in the added interference. Therefore, notch filter should have two notches to attenuate the interference as described in real sinusoidal under chapter 2. The notch details are presented in Table 3.8.

Table 3.8: Notch details for unity 3-D degraded image

θ_1	r_1	θ_2	r_2	θ_3	r_3
0.2π	0.5	0.4π	0.5	0.6π	0.5
-0.2π	0.5	-0.4π	0.5	-0.6π	0.5

Figure 3.18 depicts the degraded image with interference, recovered image using M-D multi-notch filter and residual (error) image of the 50th plane of the unity 3-D image. The error image is the error between unity 3-D image input and recovered image. SIR is calculated for input

and output images in order to measure the effectiveness of the interference attenuation using equation (4) and (5).

$$SIR_{before} = \frac{\sum_{l=26}^{75}\sum_{m=26}^{75}\sum_{n=26}^{75}(v)^2}{\sum_{l=26}^{75}\sum_{m=26}^{75}\sum_{n=26}^{75}(x-v)^2} \tag{18}$$

$$SIR_{after} = \frac{\sum_{l=26}^{75}\sum_{m=26}^{75}\sum_{n=26}^{75}(y)^2}{\sum_{l=26}^{75}\sum_{m=26}^{75}\sum_{n=26}^{75}(y-v)^2} \tag{19}$$

Where v, x and y are original, degraded and recovered 3-D images respectively.

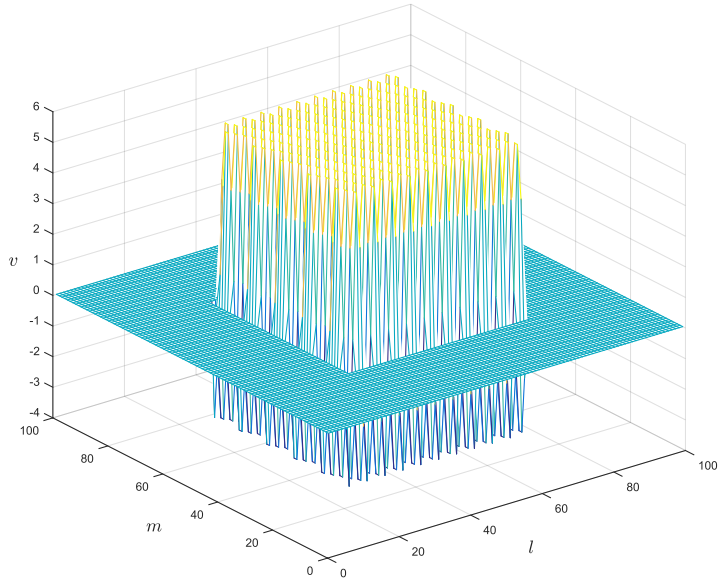

(a)

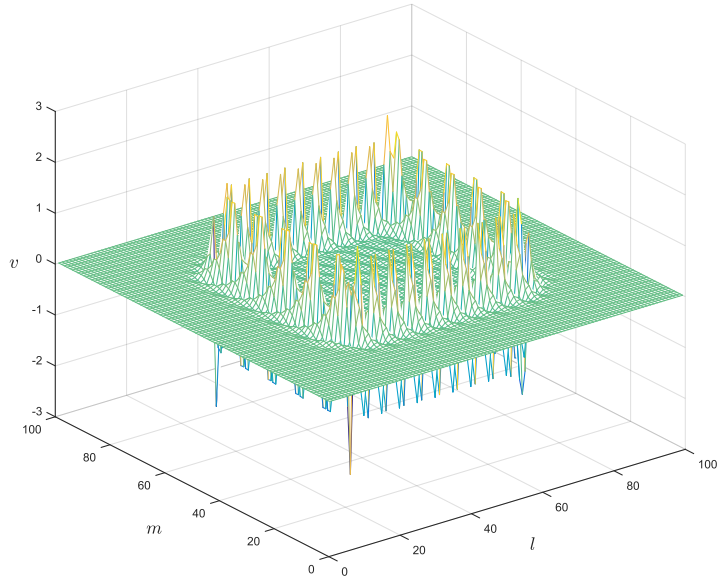

(b)

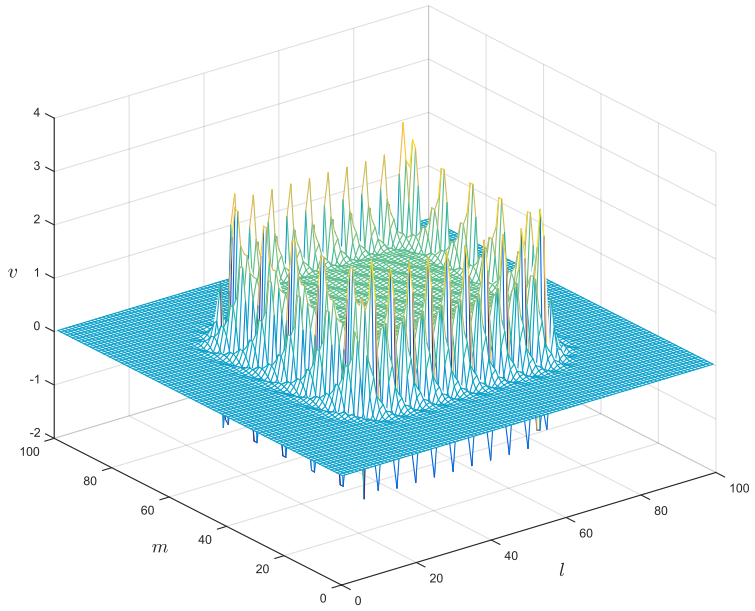

(c)

Figure 3.18: (a) Degraded Image; (b) Error Image; (c) Recovered image

The improved SIR of the signal with comparison Piyachaiyakul's method is illustrated in Table 3.9. It is clearly identified that proposed M-D multi-notch filter attenuate SIR is higher than existing IIR notch filtering method. Figure 3.19 illustrates the SIR variation along with amplitude. It can be clearly identified that Piyachaiyakul's method has moreover constant SIR for all the tested amplitudes of the interference signal. However, the proposed M-D IIR multi notch filtering method has increase interference attenuation with increased amplitude of the interference signal.

Table 3.9: Improved SIR of the proposed IIR notch filter

Amplitude A	SIR_{before} (dB)	SIR_{after} (dB)	$SIR_{improved}$ (dB)	$SIR_{Piya's\ method}$ (dB)
0.5	9.0309	21.0782	12.0473	10.9209
1	3.0103	16.5493	13.5390	10.9222
5	-10.9691	4.7983	15.7674	10.9695
10	-16.9897	1.7810	18.7707	11.1145
15	-20.5115	0.8831	21.3946	11.3458
20	-23.0103	0.5188	23.5291	11.6503
30	-26.5321	0.2383	26.7704	12.4183

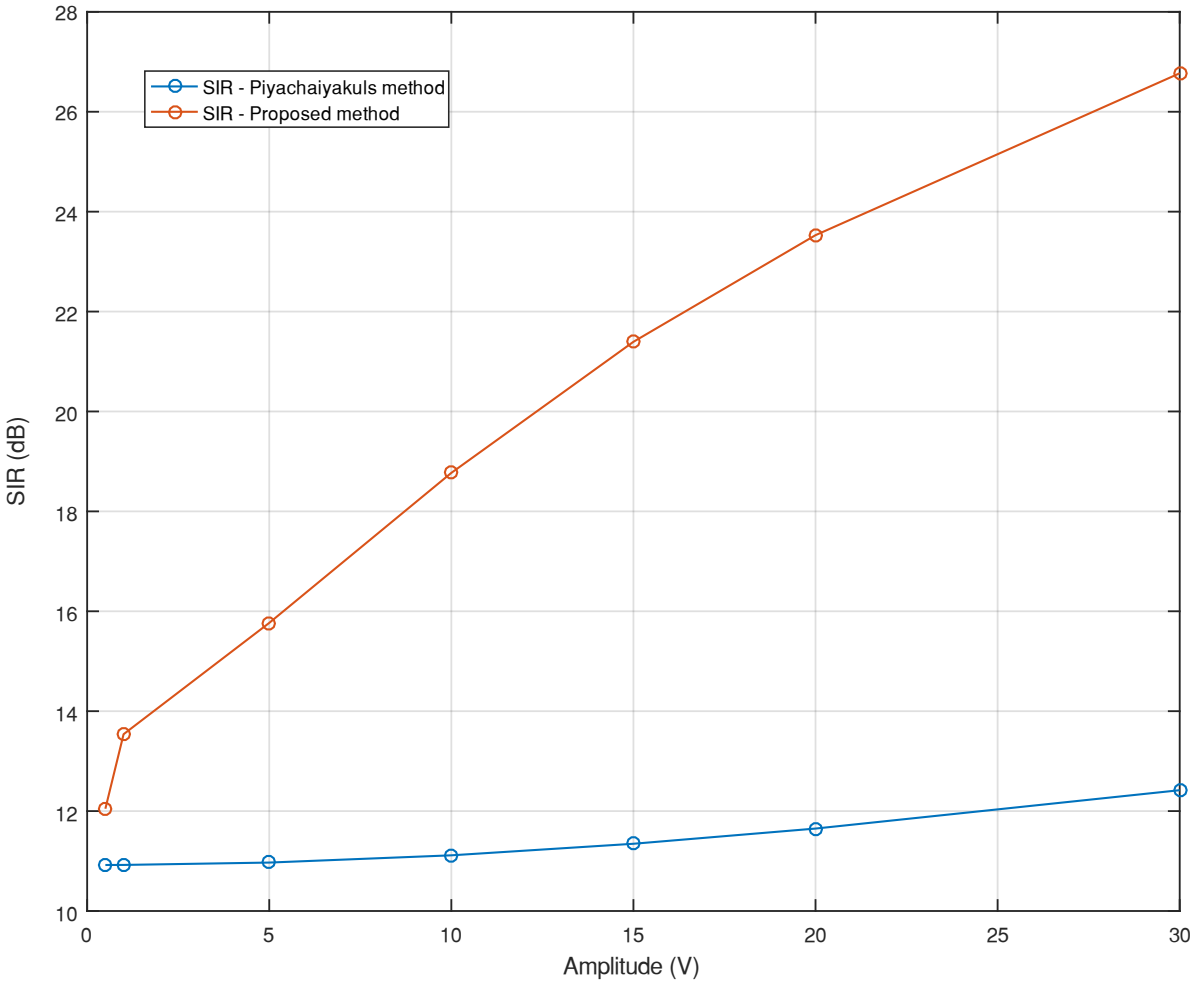

Figure 3.19: SIR comparison

4. CONCLUSION AND FUTURE WORK

4.1. Conclusions

In this dissertation, M-D IIR multi-notch filter has been introduced. There are few researches have been carried out in this regard and only limited to 3-D single notch. However, due to the lack of flexibility such as number of notches and notch placement, a new generalised notch filter framework has been introduced. The key factor of the proposed notch filter is the flexibility of placing the notches and adding any number of notches.

It can be clearly identified that the magnitude response doesn't have a smooth shape in the notch in the previous studies. However, the magnitude response of the proposed method has a proper shape compared to the previous studies. Thus, helps the proposed notch filter to supress the specified frequency without changing the input signal. The phase of the output signal is similar to the phase of the input signal due to the zero phase characteristics of the proposed IIR notch filter.

Interference that is introduced in the experiments, are real-valued. However, there will be complex interference exists in the signals and the proposed IIR notch filter is capable of filtering out both real and complex parts.

Stability of the filter is an important factor to consider. The structure of the notch filter is closed-form and it is always BIBO stable.

The proposed filter capabilities are compared against the existing filtering method. It is clearly noticeable that, the proposed M-D multi notch IIR filter has better performance as well as greater flexibility.

4.2. Future work

There are certain factors can be identified as future work of this study. The implementation is done only in the software at the moment of writing of this dissertation. The proposed notch filter can be implemented on hardware so that it can be useful for many applications.

The experiments are carried out by adding the notch details manually. It is better to develop an algorithm to identify the frequencies automatically and make an adaptive notch filter. That will be huge time saving task.

There is a transient in the filtered signal and padding is used to hide that. There are some techniques developed for transient suppression. Therefore, using those techniques might reduce the amount of transient thus the amount of padding can be eliminated or kept at minimum level in a future study.

REFERENCES

[1] M. D. Adams, Continuous-Time Signals and Systems, Canada: University of Victoria, 2013.

[2] G. Berntson and J. Cacioppo, Handbook of Neuroscience for the Behavioral Sciences, Wiley, 2009.

[3] M. Levoy and P. Hanrahan, "Light field rendering," in *in Proceedings of Annual Conference on Computer Graphics (SIGGRAPH)*, pp 31-42, 1996.

[4] C. U. S. Edussooriya, "Low-Complexity Multi-Dimensional Filters for Plenoptic Signal Processing," PhD thesis, Department of Electrical and Computer Engineering, University of Victoria, Victoria, BC, Canada, 2015.

[5] C. U. S. Edussooriya, D. G. Dansereau, L. T. Bruton and P. Agathoklis, "Five-dimensional depth-velocity filtering for enhancing moving objects in light field videos," *IEEE Transactions on Signal Processing*, vol. 63, no. 8, p. 2151–2163, 2015.

[6] E. Adelson and J. Bergen, "The plenoptic function and the elements of early vision," *in Computation Models of Visual Processing (M. Landy and J. A. Movshon, eds.),* pp. 3-20, 1991.

[7] S. Pulipati, V. Ariyarathna, A. Madanayake, R. Wijesekara, C. U. S. Edussooriya and L. Bruton, "A 16-element 2.4-GHz multi-beam array receiver using 2-D spatially-bandpass digital filters," *IEEE Transactions on Aerospace and Electronic Systems,* vol. 55, no. 6, pp. 3029-3038, Dec 2019.

[8] T. K. Gunaratne and L. T. Bruton, "Broadband beamforming of bandpass plane waves using 2D FIR trapezoidal filters at baseband," in *IEEE Asia Pacific Conference on Circuits and Systems*, Singapore, 2006.

[9] S. Pulipati, V. Ariyarathna, A. Jayaweera, C. U. S. Edussooriya, C. Wijenayake, L. Belostotski and A. Madanayake, "FPGA-based 2-D FIR Frost beamformers with digital mutual coupling compensation," in *IEEE/MTT-S International Microwave Symposium (IMS)*, Los Angeles, 2020.

[10] T. Gunaratne and L. Bruton , “Adaptive complex-coefficient 2D FIR trapezoidal filters for broadband beamforming in cognitive radio systems,” *Circuits, Systems, and Signal Processing,* vol. 30, no. 3, pp. 587-608, Mar 2011.

[11] H. L. Van Trees, Optimum array processing, John Wiley & Sons, 2004.

[12] M. De Carvalho, M. Pereira, G. Alves, E. Silva, C. Pagliari, F. Pereira and V. Testoni, “A 4-D DCT-Based lenslet light field codec,” in *IEEE International Conference on Image Processing*, Athens, 2018.

[13] N. Liyanage, C. Wijenayake, C. U. S. Edussooriya, A. Madanayake, R. Cintra and E. Ambikairajah, “Low-complexity real-time light field compression using 4-D approximate DCT,” in *IEEE International Symposium on Circuits and Systems*, Seville, 2020.

[14] Y. Miyagi, K. Takahashi, M. Tehrani and T. Fujii, “Reconstruction of compressively sampled light fields using a weighted 4D-DCT basis,” in *IEEE International Conference on Image Processing*, Quebec City, 2015.

[15] V. Srivastava and G. Ray, “Design of 2D-multiple notch filter and its application in reducing blocking artifact from DCT coded image,” in *Proceedings of the 22nd Annual International Conference of the IEEE Engineering in Medicine and Biology Society*, Chicago, 2000.

[16] N. Piyachaiyakul and C. Charoenlarpnopparut, “Non-separable three-dimensional IIR notch filter design using outer product expansion,” *IEEE Transactions on Circuits and Systems—II ,* vol. 58, no. 9, pp. 605-609, 2011.

[17] Q. Wang and D. Kundur, “A generalized design framework for IIR digital multiple notch filters,” *EURASIP Journal on Advances in Signal Processing,* 2015.

[18] J. Piskorowski, “Digital Q-varying notch IIR filter,” *IEEE Transactions on Instrumentation and Measurement ,* vol. 59, pp. 866-872, 2010.

[19] S.-C. Pei and C.-C. Tseng, “Two dimensional IIR and FIR digital notch filter design,” in *IEEE International Symposium on Circuits and Systems,* Chicago, 1993.

[20] S.-C. Pei, W.-S. Lu and C.-C. Tseng, “Analytical two-dimensional IIR notch filter design using outer product expansion,” *IEEE Transactions on Circuits and Systems—II: Analog and Digital Signal Processing* , vol. 44, no. 9, September 1997.

[21] S.-C. Pei, B.-Y. Guo, W.-Y. Lu, G. E. Sobelman and Y.-D. Huang, “Improved design of digital 1-D and 2-D notch filters using general feedback structure,” in *IEEE International Symposium on Circuits and Systems* , Montreal, QC, Canada, 2016.

[22] A. Chinoun, L. Mitiche and A. B. H. Adamou-Mitiche, “New design approach of three-dimensional IIR notch filter using all-pass sections,” *Australian Journal of Electrical and Electronics Engineering,* vol. 16, no. 4, pp. 276-280, 2019.

[23] L. Tan and J. Jiang, “Digital signal processing: fundamentals and applications,” Elsevier Inc, 2013, pp. 365-366.